Eur. Phys. J. D **9**, 331–335 (1999)

THE EUROPEAN PHYSICAL JOURNAL D
EDP Sciences

Radiative cooling of C_{60} and C_{60}^+ in a beam

A.A. Agarkov[1], V.A. Galichin[1], S.V. Drozdov[1], D.Yu. Dubov[1,2], and A.A. Vostrikov[1,2]

[1] Institute of Thermophysics SB RAS, Novosibirsk 630090, Russia (e-mail: vostrikov@itp.nsc.ru)
[2] Novosibirsk State University, Novosibirsk 630090, Russia

Received: 31 August 1998 / Received in final form: 10 November 1998

Abstract. We observed a continuous emission spectrum of C_{60}^* and C_{60}^{+*} clusters induced by electron impact for wavelengths 300 to 800 nm (the monochromator's resolution was $\Delta\lambda = 3.2$ nm). The emission spectrum was described by a modified Planck's formula for the black-body-like radiation. The radiative temperature of clusters, T, (up to 3100 K) and the integral intensity of emission depend on the electron energy E_e in a beam. The intensity of emission from C_{60}^+ is higher than that from a neutral cluster. The emissivity coefficient has been found to be $\varepsilon(C_{60}^{+*}) = 7.6 \times 10^{-3}$.

PACS. 34.80.Gs Molecular excitation and ionization by electron impact – 61.48.+c Fullerenes and fullerene-related materials – 78.60.-b Other luminescence and radiative recombination

1 Introduction

The cluster of C_{60} is a unique object for fundamental and applied investigations. The high stability and the low number of atoms in a C_{60} cluster facilitate its use in the study of a fundamental phenomenon: the formation of a unified quantum-mechanical system (solid phase) from separate atoms.

In our previous works, we have studied the radiation of particles (clusters of molecular gases $(CO_2)_n$, $(N_2O)_n$, $(H_2O)_n$, and $(N_2)_n$) formed in supersonic jets and excited by an electron impact [3–5]. It was established that the energy of vibrational [3], and electronic [4, 5] excitation transfers rapidly into heat. The decay rate of excited states drastically increases with the cluster size, and the emission spectrum corresponds to the electron-excited states of molecules which leave the cluster.

As for strongly bound clusters (such as clusters of refractory substances), their radiative cooling occurs with a continuous black-body-like spectrum observed for clusters of $(Nb)_n$ [6] ($n \approx 260$, radiative temperature is up to 3200 K), and for C_{60} [7, 8]. In [7], C_{60} clusters were evaporated from the solid phase into vacuum by laser radiation, and the thermal emission spectrum in the region of 360–750 nm was observed. In [8], a fullerene was excited by electron impact in an effusive beam.

In this work, the black-body-like emission was induced by the electron beam crossing the beam of C_{60} clusters. We established that the emission is associated mainly with charged clusters of C_{60}^+. The results of [6–8] and this work indicate that the way of excitation does not influence the emission spectra of the clusters. This means that the black-body-like radiation is the property of strongly bound clusters.

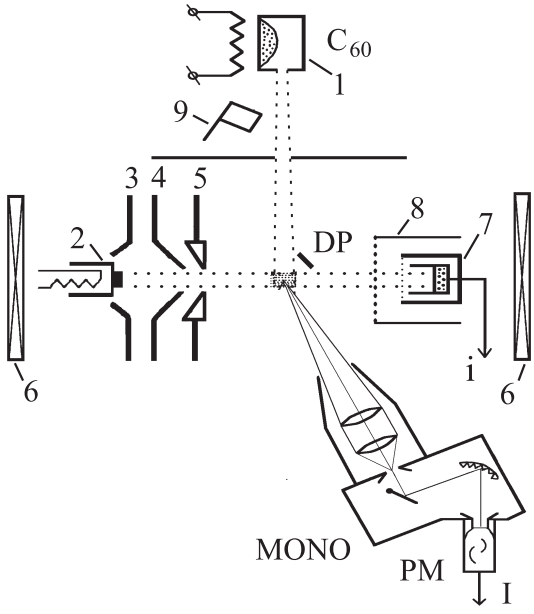

Fig. 1. Experimental setup.

2 Experimental technique

The scheme for generation of a C_{60} cluster beam and excitation with an electron beam was the same as that in experiments measuring absolute cross sections of C_{60}^- [1, 9] and C_{60}^+ [2, 9]. A schematic diagram of the experimental apparatus, supplemented by an optical system, is given in Fig. 1.

In this work, we employed a mixture of fullerenes, C_{60}/C_{70}, obtained by Krätschmer's method. The C_{60} con-

tent measured in the gas phase by a time-of-flight mass-spectrometer was larger than 88%. The fullerene vapor, effusing from a cylindrical source 1, heated up to $T_0 \approx 800$ K and was intersected by the electron beam at an angle of 90°. The beam-crossing region had the shape of a cylinder 2.5 mm in diameter and 15 mm long, oriented parallel to the electron beam.

The beam of electrons that emitted from an oxide-coated cathode 2 was shaped by a system of diaphragms 3–5 and collimated by a magnetic field (≤ 300 G) of magnets 6. The electron current measured by a Faraday cup 7 did not exceed 60 μA, which ensured the binary character of the electron–cluster interaction. The electron energy E_e varied from 0 to 100 eV.

The emission from the beam-crossing region was detected at right angles to the electron beam; the angle with the direction of the molecular beam was equal to 40°. With short-focal objective lenses, the emission was focused onto the input slit of a grating monochromator (MONO) (200–800 nm, inverse dispersion 3.2 nm/mm) and after spectral decomposition, it was recorded with a photomultiplier (PM). A calibrated quartz-tungsten lamp was used to obtain the relative spectral efficiency of the entire optical system. The raw spectra corrected by this response curve gave a photon flux, I, to PM. Replacing the monochromator by a broadband filter, we collected the total emission signal.

In order to separate the contribution to the emission of C_{60}^* neutrals from C_{60}^{+*} ions, we applied an electric field between two deflecting plates (DP) placed along the axes of both molecular and electron beams. Having been extracted, the ions became undetectable for the registration system, thus the residence time of ions in the observation region, t, was reduced with increasing voltage. The magnetic collimation ensured that the applied electric field had no influence on the electron beam. To test this fact, we measured in the same scheme the radiation of an N_2^+ ion ($B^2\Sigma_u$, $\lambda = 391$ nm). The radiation of this short-lived state was independent from the extracting field.

In general, both charged and neutral fragments (C_{60-2n}^+ and C_{60-2n}^*) may also contribute to the measured radiation. But we should take into account that the stability of the C_{60} fullerene reduces strongly the dissociative processes at the electron impact, so that the threshold of fragmentation is shifted to 42–44 eV, and the contribution of fragments to the total ionization cross section at $E_e \leq 100$ eV does not exceed 5%–7% [10, 12]. This is indirect evidence that the radiation was mainly caused by the undissociated particles.

We excluded the possibility that other sources of radiation produced undesirable secondary effects: The contribution of the electron-induced radiation from the background gas was monitored with the aid of an electromagnetic shutter 9, which can cut off the molecular beam. We eliminated the possible IR background from the heated parts of the fullerene source by operating in a regime of modulation of the electron beam. For this purpose, the electron beam was interrupted with a frequency of 80 Hz, and the signal from the PM was measured in a lock-in mode.

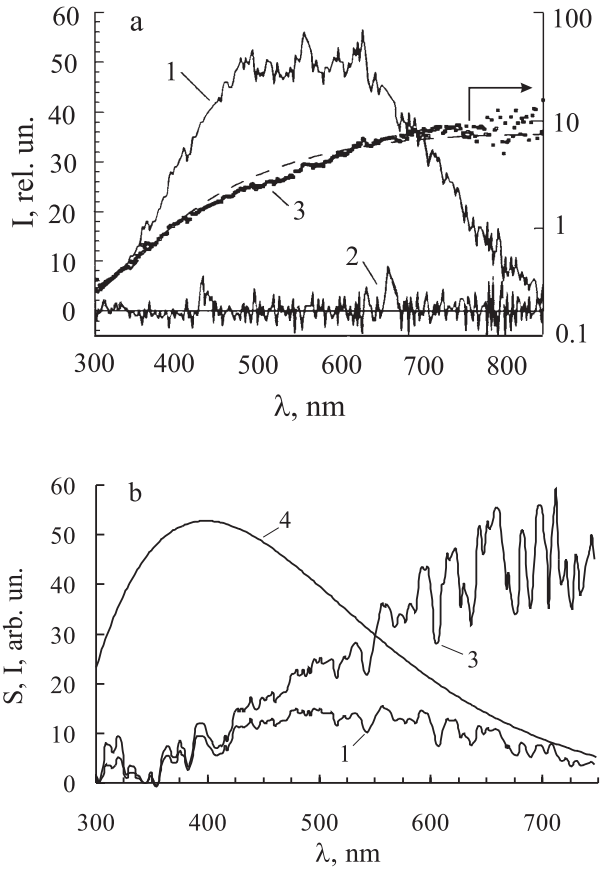

Fig. 2. Optical emission from fullerene beam. Raw spectra of fullerene (1) and background gas (2), corrected spectrum of fullerene radiation (3), and spectral efficiency of optical system (4).

3 Results and discussion

Figure 2a,b shows the spectra of radiation (curve 3) produced by electron impact with a C_{60} cluster in crossed beams. The spectra were recorded with 66-eV (Fig. 2a) and 30-eV 6(Fig. 2b) electrons. The emission spectrum was obtained as the difference between the total PM signal and the emission of the background gas. Thereafter, this difference (curve 1) was normalized to the total spectral efficiency of the detecting system, S.

One can see that the spectra of a fullerene beam have quasi-continuous character. In view of the large number of radiating modes, the form of the spectrum is determined not by the structure of the vibrational levels but rather only by the internal temperature of the molecules. Therefore it is of interest to compare this spectrum with the modified Planck's radiation spectrum of a small body heated up to some temperature T. The rate of photon emission K_r in the wavelength interval $[\lambda, \lambda + \Delta\lambda]$ by a heated sphere is

$$K_r(\lambda, T) = 2\pi c S \Delta\lambda \varepsilon(\lambda, T)/[\lambda^4(\exp(hc/\lambda kT) - 1)], \quad (1)$$

where $S = \pi d^2$ is the surface area, d is the diameter of the C_{60} ball (0.7 nm), and $\varepsilon(\lambda, T)$ is the emissivity coefficient of

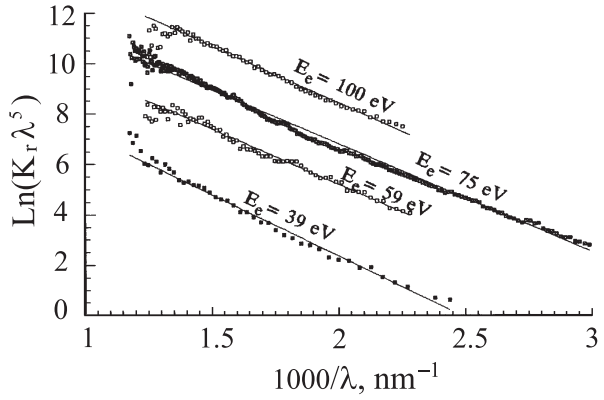

Fig. 3. Emission spectra in $\ln(K_r\lambda^5) - \lambda^{-1}$ coordinates.

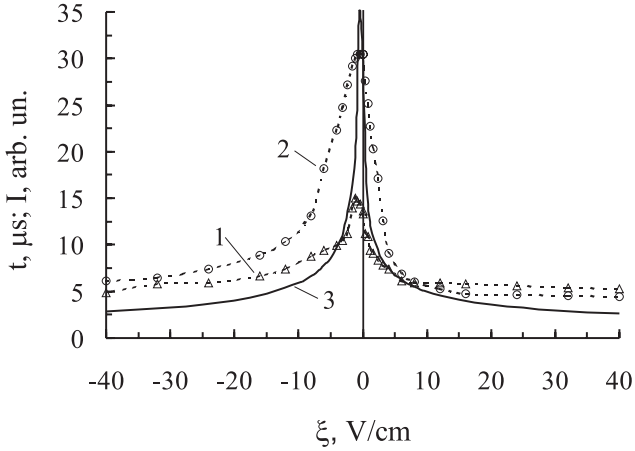

Fig. 4. Radiation at $E_e = 40$ eV (1) and $E_e = 65$ eV (2), and the average residence time of a C_{60}^+ ion in the detection region (3) vs. the extracting field ξ.

the body. From general considerations [11], the emissivity for $d \ll \lambda$ should be $\leq d/\lambda$. We set for a while $\varepsilon(\lambda) = d/\lambda$. For the visible and near-IR spectra, the photon energy is much greater than kT, and therefore we obtain from (1) the following

$$K_r(\lambda, T) \sim \lambda^{-5} \cdot \exp(-hc/\lambda kT). \qquad (2)$$

The black-body emission spectrum calculated from (2) for $T = 3141$ K is shown in Fig. 2a with a dashed curve.

In Fig. 3, the results of the spectral measurements performed with different electron energies E_e are presented in the form of plots of $\ln(K_r \cdot \lambda^5)$ versus λ^{-1}. One can see that the results are approximated well by straight lines, whose slope, according to (2), equals hc/kT. Closer inspection shows that some experimental spectra in Fig. 3 seem to have a weak positive curvature which might be corrected by a proper choice of the emissivity coefficient $\varepsilon(\lambda, T)$. We took the more common approximation of $\varepsilon(\lambda, T)$ in the form $(d/\lambda)^n$ and tried to get better linearity by the variation of n. All of the measured spectra were found to have the least deviation from the Planck approximation at n ranging from 0.5 to 2. Thus, by choosing $n = 1$, we seem

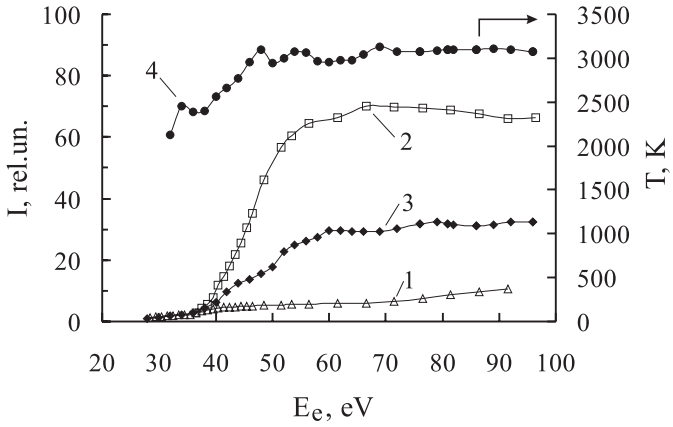

Fig. 5. Radiation intensity (1–3), and radiation temperature (4) vs. E_e. Total emission of C_{60}^* (1); total (2) and selected ($\lambda = 540$ nm, $\Delta\lambda = 3.2$ nm) (3) emission of both C_{60}^* and C_{60}^{+*}.

to use a reasonable approximation. At the same time, one should remember that the power n influences the extracted radiation temperature: $T(n = 0.5) \approx 1.07 \cdot T(n = 1)$ and $T(n = 2) \approx 0.9 \cdot T(n = 1)$.

Figure 4 shows the total emission signal (the intensity of the PM signal when the optical system with a broad filter collects the total emission signal) depending on the strength and polarity of electric field ξ between DP.

This figure also shows the time of the detection of C_{60}^+ radiation versus ξ (curve 3). This time has been calculated for the ion formed at the center of the electron beam, with the vector of initial thermal velocity of C_{60} directed, at the angle of 40°, to the optical system axis. This angle causes the asymmetry of the curves. In Fig. 4, one can see that the ions contribute mainly to the emission signal I.

The emission signal as a function of electron energy for different experimental conditions is shown in Fig. 5. Here curve 1 corresponds to the total emission of the neutral C_{60}^* clusters ($\xi = 12$ V/cm). Curves 2 and 3 show the emission of C_{60}^* and C_{60}^{+*} ($\xi = 0$ V/cm).

Measuring the ratio of the emission signals for different wavelengths (450 to 700 nm) and describing the spectrum of the emission with Planck's law, we obtained the cluster temperature T, which depends on the electron energy (curve 4 in Fig. 5). It can be seen that initially the relationship $T(E_e)$ increases proportionally with E_e, but at $E_e \approx 47$ eV, it reaches the maximum value, $T_m \approx 3100$ K. This value of T_m corresponds to the internal energy of a cluster C_{60} $E_v \approx 36$ eV (the initial internal energy of the cluster at $T_0 = 800$ K is $E_{v,0} \approx 4.6$ eV [12]).

The existence of a maximum value T_m may be explained by the competition between radiative cooling of the electron-heated cluster and other cooling processes, such as the evaporation of fragments and dissociative ionization. Note that the sum $kT_m + U_i$, where U_i is the ionization energy threshold for C_{58}, was about the same value as the appearance energy of dissociative ionization: $C_{60} + e^- \rightarrow C_{58}^+ + C_2 + 2e^-$ [10, 12].

Figure 6 shows the emission rate at the energy $E_e = 65$ eV for the C_{60}^{+*} ion, K_r^+, as a function of ion travel

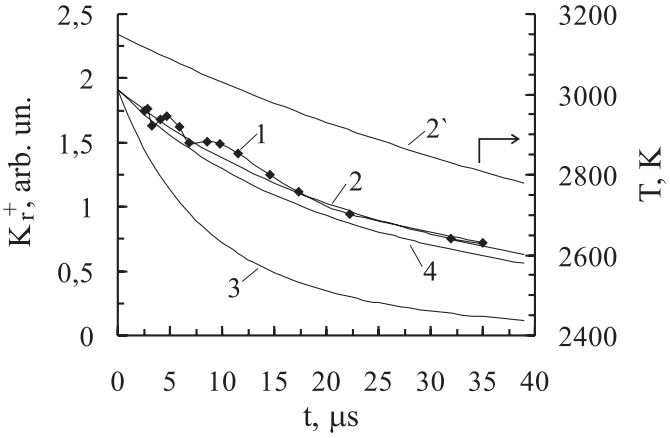

Fig. 6. The radiation rate (1–4) and the temperature (2′) of C_{60}^{+} ion depending on the residence time of ion. (1): experiment; (2–4): fitting calculations.

time to the deflecting plate (curve 1). These points were obtained from the data shown in Fig. 4 (curve 2). The procedure was as follows. We subtracted the contribution of C_{60}^{*} emission from the overall emission intensity of C_{60}^{*} and C_{60}^{+*}. (The contribution of C_{60}^{*} was obtained by extrapolation of the $I(t)$ dependence to $t = 0$. The value of $I(C_{60}^{*})$ comes to only 3% of the overall intensity.) Then, for every time moment t in Fig. 4, the obtained emission signal was divided by the average ion density n^{+} in the observed range. The dependence of n^{+} on t was determined from the balance equation of clusters fluxes through borders of observation region.

One can see in Fig. 6 that the curve for $K_r^{+}(t)$ decreases with t. This decrease is obviously connected with the radiative cooling of a C_{60}^{+*} cluster. In order to obtain the dependence of emission intensity on the cooling rate, we integrated the radiation energy flux $q = (hc/\lambda)K_r$ over λ. Let us assume that the emissivity coefficient is

$$\varepsilon(\lambda, T) = \varepsilon_0 \cdot \varepsilon(\lambda) \cdot \varepsilon(T), \tag{3}$$

where $\varepsilon(\lambda) = d/\lambda$, $\varepsilon(T) = (T/T_\varepsilon)^{\alpha}$, and ε_0, T_ε, α are constants.

After integrating over λ we obtain

$$q = \varepsilon_0 \cdot \varepsilon(T) \cdot \sigma_c \cdot T^5, \tag{4}$$

where $\sigma_c = 24.888 \cdot 2\pi hc^2 Sd(k/hc)^5$.

Since $q \cdot \mathrm{d}t = -C \cdot \mathrm{d}T$, where the heat capacity for our temperature range is $C = \mathrm{d}E/\mathrm{d}T = 0.0143\,\mathrm{eV/K}$ [12], one can integrate over time and temperature and obtain the time dependence of the cluster temperature due to black-body-like emission

$$T(t, T_i) = T_i \cdot \left\{ 1 + t \cdot \frac{(4+\alpha)\varepsilon_0 \sigma_c T_i^{4+\alpha}}{C T_\varepsilon^{\alpha}} \right\}^{-1/(4+\alpha)}, \tag{5}$$

where T_i is the initial temperature of the C_{60}^{+*} cluster.

Substituting (5) into (1), we derive the expression for the emission intensity K_r^{+} as a function of temperature T_i and time t. Curves 2–4 in Fig. 6 represent the results of the K_r^{+} calculations. Here is $T_\varepsilon = T_i = 3150\,\mathrm{K}$, $\lambda = 550\,\mathrm{nm}$. The constants are $\alpha = 0$ and $\varepsilon_0 = 6$ (curve 2), $\alpha = 0$ and $\varepsilon_0 = 20$ (curve 3), $\alpha = 2$ and $\varepsilon_0 = 6$ (curve 4).

The calculations revealed that the change from $\alpha = 0$ to $\alpha = 2$ does not make any qualitative change in the dependence $K_r^{+}(t)$. This $K_r^{+}(t)$ dependence is more sensitive to changing ε_0. Therefore we can propose that the emissivity coefficient ε_0 is the only fitting parameter. Considering that curves 1 and 2 are in agreement (Fig. 6), let us take $\varepsilon_0 = 6$. Then, assuming $\alpha = 0$ in (5), we obtain for C_{60}^{+*} that $\varepsilon^{+} = 7.6 \times 10^{-3}$. The result of the calculation of C_{60}^{+*} cooling by black-body-like radiation according to (5) is shown in Fig. 6 with curve 2′.

Several groups have previously obtained the emissivity coefficients of fullerene species by analyzing the effect of radiative cooling on some processes. These data are summarized in Table 1.

Table 1. The comparison of the available data on the emissivity coefficients ε. EIF: electron-induced fragmentation; MSF: metastable fragmentation; TIE: thermionic emission; PE: photon emission.

Species	ε	Studied process	Reference
C_{60}^{*}	$(3-8)\times 10^{-5}$	EIF	[12]
C_{60-2n*}^{+}	$\sim (0.4-3)\times 10^{-3}$	MSF	[13]
C_{60}^{-*}	$\sim 1.3\times 10^{-4}$	TIE	[14]
C_{60}^{+*}	7.6×10^{-3}	PE	this work

4 Conclusions

The clusters C_{60}^{*} and C_{60}^{+*} heated by electron impact are able to emit heat radiation in a continuous spectrum like a black body.

This work was supported by the Russian Foundation for Basic Research (grants 97-02-18510 and 98-02-17804) and a grant from the Education Ministry of the Russia Federation.

References

1. A.A. Vostrikov *et al.*: Molec. Mater. **20**, 255 (1998)
2. A.A. Vostrikov, D.Yu. Dubov, A.A. Agarkov: Tech. Phys. Lett. **21**, 715 (1995)
3. A.A. Vostrikov, S.G. Mironov: Chem. Phys. Lett. **101**, 583 (1983)
4. A.A. Vostrikov, D.Yu. Dubov, V.P. Gilyova: Z. Phys. D **20**, 205 (1991)
5. A.A. Vostrikov, V.P. Gileva: Tech. Phys. Lett. **20**, 625 (1994)
6. V. Frenzel, A. Roggenkamp, D. Kreisle: Chem. Phys. Lett. **240**, 109 (1995)
7. R. Mitzner, E.E.B. Campbell: J. Chem. Phys. **103**, 2445 (1995)

8. A.A. Vostrikov, D.Yu. Dubov, A.A. Agarkov: JETP Lett. **63**, 963 (1996)
9. A.A. Vostrikov, D.Yu. Dubov, A.A. Agarkov: Tech. Phys. Lett. **21**, 517 (1995)
10. M. Foltin *et al.*: J. Chem. Phys. **98**, 9624 (1993)
11. C.F. Bohren, D.R. Huffman: *Absorption and Scattering of Light by Small Particles* (Wiley, New York 1983)
12. E. Kolodney, B. Tsipinyuk, A. Budrevich: J. Chem. Phys. **102**, 9263 (1995)
13. K. Hansen, E.E. Campbell: J. Chem. Phys. **104**, 5012 (1996). The products $\varepsilon_n \cdot D_n$ were obtained. We assume that the evaporative activation energies D_n are in 4–8 eV range.
14. J.U. Andersen *et al.*: Phys. Rev. Lett. **77**, 3991 (1996)